

van der Waals equation of state for a fluid in a nanopore

Guillermo J. Zarragoicoechea and Víctor A. Kuz

IFLYSIB (UNLP, CONICET, CICPBA), casilla de correo 565, 1900 La Plata, Argentina

(Received 6 July 2001; published 24 January 2002)

A generalization of the van der Waals equation of state is presented for a confined fluid in a nanopore. The pressure in the fluid, confined in a narrow pore of infinite length, has tensorial character. From this hypothesis, the Helmholtz free energy is constructed and expressions for the axial and transversal components of the pressure tensor are obtained. The equations predict liquid-vapor equilibria, and a shift of the critical point with respect to that obtained from the van der Waals bulk equation. The results are in good agreement with recent experiments.

DOI: 10.1103/PhysRevE.65.021110

PACS number(s): 64.10.+h, 64.70.Nd, 05.70.Fh

I. INTRODUCTION

There is a vast knowledge about phase transitions in bulk fluids. When in a given thermodynamic system the volume is reduced to microscopic levels, the equilibrium between phases is no longer size independent. Confinement changes the thermodynamic character of the fluid [1]. The pressure is a diagonal tensor, and should be used in the description of fluids at the microscopic and mesoscopic scales when equilibrium between phases is analyzed.

The behavior of the fluid within a pore is of fundamental importance in many fields. The determination of mesopore diameters or micropore volumes in a solid [2], the pressure in a fluid confined in a cell membrane, and the behavior of water in a channel of proteins where solutes (inorganic ions) pass through the cell membranes [3] are problems of practical and theoretical interest. In this context it is important to mention the Kelvin equation, or some of the modern versions of this equation [4–6], which predict the adsorbed layer thickness or the transition from capillary to multilayer adsorbed phase inside the pore.

In tribology, the science of friction at the microscopic scale [7], the phenomenon of dissipation of energy is of much concern. In a mechanically confined fluid, the energy dissipated by friction can induce chemical transformations, liquid-gas phase transitions, or drastic changes of static and dynamic properties like shear stress, coefficient of friction, compressibility, and viscosity. These dynamic and static properties can no longer be described even qualitatively in terms of the bulk properties [8].

Liquids confined between two surfaces or within a narrow space with dimensions smaller than 5–10 molecular diameters become ordered into layers, and within each layer they can also have lateral order. Across molecularly thin films of simple liquids, there is a structuring of the molecules and an exponentially decaying oscillatory force, varying between attraction and repulsion with a periodicity of the order of the solvent molecular dimension [9]. A similar result is found in polymeric thin films in relation to the density, which exhibits gradually decaying oscillations [10]. A lattice-gas cellular automata model of porous media constructed at the pore scale predicts formation of a microscopic liquid film condensed on the solid walls in equilibrium with the gas phase

[11]. All these analyses tacitly show that a fluid in a nanopore has tensorial character.

Equilibrium and nonequilibrium experiments show that a confined fluid behaves differently from the corresponding bulk fluid. The relaxation rate of ethylene glycol versus temperature is different in a zeolite host system from the bulk fluid [12]. In pure liquid (sulfur hexafluoride), the experiments of Thommes and Findenegg [13] determined the critical point shift in three kinds of controlled-pore glass. A direct determination of the phase coexistence properties of fluids by Monte Carlo simulation predicts the adsorption and capillary condensation of a simple fluid (Ar) in narrow cylindrical pores (CO₂). The gas-liquid critical temperature decreases as the pore radius is reduced [14]. The same phenomenon was observed in liquid-liquid phase equilibria by Sliwinska-Bartkowiak *et al.* [15]. Here the effect of confinement produced a lowering of the critical mixing temperature and a shift in the critical mixing composition.

In relation to this general presentation, we study the problem of confined fluids in a narrow pore via an extension of the van der Waals equation. The phase transitions, shift of the critical point, and critical temperatures predicted by this theory are in good agreement with the results of experiments and numerical simulations.

II. VAN DER WAALS EQUATION FOR A CONFINED FLUID

We assumed that the pressure in a confined fluid is a diagonal tensor $\hat{\mathbf{P}}$ with components p_{ii} ($i=x,y,z$). The internal energy is given by [16]

$$dE = T dS - \sum_i p_{ii} d\epsilon_{ii} V, \quad (1)$$

where the second term on the right-hand side represents the work done by the internal tension under a specific deformation $d\epsilon_{ii}$ of the volume V . From the Helmholtz free energy $F = E - TS$ we obtain

$$dF = -S dT - \sum_i p_{ii} d\epsilon_{ii} V \quad (2)$$

with the components of $\hat{\mathbf{P}}$ given by

$$p_{ii} = -\frac{1}{V} \frac{\partial F}{\partial \epsilon_{ii}}. \quad (3)$$

The Helmholtz free energy of a system of N particles interacting via a pair potential $U(r_{12})$ (inert walls) can be written as

$$F = F_0 - \frac{kTN^2}{2V^2} \int \int (e^{-U(r_{12})/kT} - 1) dV_1 dV_2, \quad (4)$$

F_0 being the free energy of the ideal gas. We consider the particles interacting via a Lennard-Jones potential $U(r_{12}) = 4\epsilon[(\sigma/r_{12})^{12} - (\sigma/r_{12})^6]$. The standard van der Waals (vdW) equation can be obtained from Eq. (4) by integrating over an infinite volume. By following the same procedure for a finite volume, we split the integral into two regions, $r_{12} < \sigma$ and $r_{12} > \sigma$:

$$F = F_0 - \frac{kTN^2}{2V^2} \left[\int \int_{r_{12} < \sigma} (e^{-U(r_{12})/kT} - 1) dV_1 dV_2 + \int \int_{r_{12} > \sigma} (e^{-U(r_{12})/kT} - 1) dV_1 dV_2 \right]. \quad (5)$$

In the first integral we approximate $e^{-U(r_{12})/kT} \approx 0$, and in the second integral $e^{-U(r_{12})/kT} \approx 1 - U(r_{12})/kT$. With these assumptions Eq. (5) becomes

$$F = F_0 + \frac{kTN^2}{V} b + \frac{kTN^2}{2V^2} \int \int_{r_{12} > \sigma} \frac{U(r_{12})}{kT} dV_1 dV_2 \quad (6)$$

with $b = \frac{2}{3} \pi \sigma^3$ and the volume $V = L_x L_y L_z$, where $L_x = L_y = L$ and $L_z = L_z$. In the thermodynamic limit, when $L_z \rightarrow \infty$ and $N \rightarrow \infty$, $\lim(L_x L_y L_z / N) = v$, the finite specific volume. By solving numerically the integral for $r_{12} > \sigma$ it is found, by fitting the results, that it can be approximated by

$$\frac{1}{V} \int \int_{r_{12} > \sigma} \frac{U(r_{12})}{kT} dV_1 dV_2 = \frac{4\epsilon}{kT} \sigma^3 I(A) \quad (7)$$

with $I(A) = c_0 + c_1/\sqrt{A} + c_2/A$. $A = L_x L_y / \sigma^2$ is the reduced area of the square section of the pore, and $c_0 = -2.7925$, $c_1 = 4.6571$, $c_2 = -2.1185$. The value of c_0 (bulk value) was obtained by solving the integral for $A = \infty$ analytically, and the values of c_1 and c_2 resulted from nonlinear fitting. The numerical values of the integral in Eq. (7) and the fitting curve $I(A)$ are represented in Fig. 1. Introducing the ideal free energy in Eq. (6) and writing $c_0 = -a/2\epsilon\sigma^3$, we have

$$F = f(T) - NkT \ln(V - Nb) + 2 \frac{N^2}{V} \epsilon \sigma^3 \left(-\frac{a}{2\epsilon\sigma^3} + \frac{c_1}{\sqrt{A}} + \frac{c_2}{A} \right), \quad (8)$$

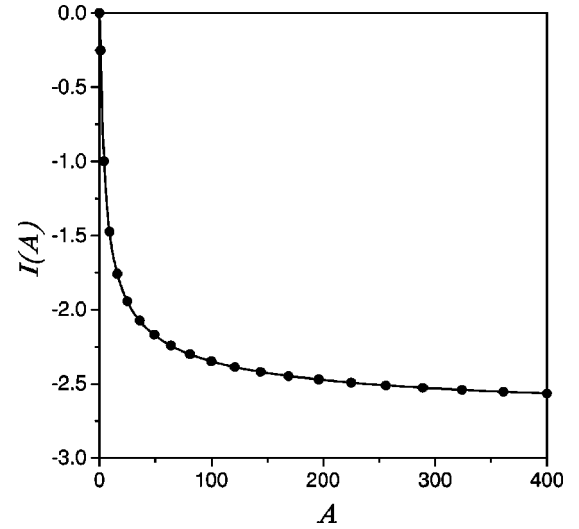


FIG. 1. Numerical values of the integral in Eq. (7) (filled circles) and the fitting curve $I(A)$ (solid line).

where we have taken into account the limited compressibility of matter by the substitution $\ln V - (N/V)b = \ln(V - Nb)$. Equation (8) represents the Helmholtz free energy of a fluid confined in an axially infinite pore of cross section A ; by using Eq. (3), we obtain the components of the pressure tensor $\hat{\mathbf{P}}$:

$$p_{xx} = p_{yy} = \frac{NkT}{V - Nb} - \frac{N^2}{V^2} \left[a - \epsilon \sigma^3 \left(3 \frac{c_1}{\sqrt{A}} + 4 \frac{c_2}{A} \right) \right], \quad (9)$$

$$p_{zz} = \frac{NkT}{V - Nb} - \frac{N^2}{V^2} \left[a - 2\epsilon \sigma^3 \left(\frac{c_1}{\sqrt{A}} + \frac{c_2}{A} \right) \right]. \quad (10)$$

Equations (9) and (10) represent the transverse and axial fluid pressures in the pore, respectively. When the cross section goes to infinity, $p_{xx} = p_{yy} = p_{zz}$, and the bulk vdW equation is recovered. In reduced coordinates, Eqs. (9) and (10) can be written as

$$p_{xx}^* = p_{yy}^* = \frac{T^*}{v^* - b^*} - \frac{a^* - [3(c_1/\sqrt{A}) + 4(c_2/A)]}{v^{*2}}, \quad (11)$$

$$p_{zz}^* = \frac{T^*}{v^* - b^*} - \frac{a^* - 2(c_1/\sqrt{A} + c_2/A)}{v^{*2}}, \quad (12)$$

with $p^* = p\sigma^3/\epsilon$, $T^* = kT/\epsilon$, $v^* = (V/N)\sigma^{-3}$, $b^* = b\sigma^{-3}$, and $a^* = a/\epsilon\sigma^3$.

From Eq. (12), the critical parameters are given by

$$T_c^* = \frac{8}{27b^*} \left(a^* - 2 \frac{c_1}{\sqrt{A}} - 2 \frac{c_2}{A} \right),$$

$$p_c^* = \frac{a^* - 2(c_1/\sqrt{A}) - 2(c_2/A)}{27b^{*2}},$$

$$v_c^* = 3b^*. \quad (13)$$

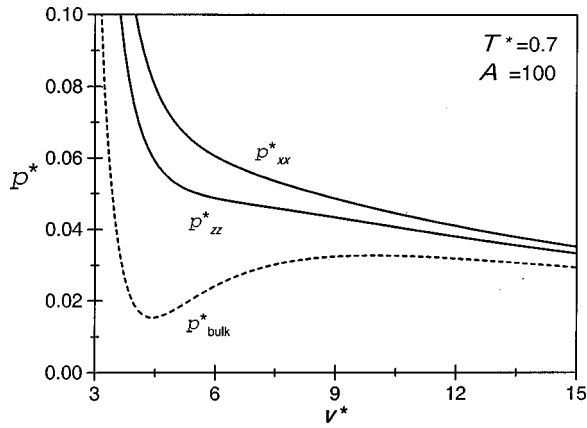


FIG. 2. Volume dependence of the pressure tensor components p_{xx} , p_{yy} , p_{zz} (full line). The bulk pressure corresponding to the same temperature is represented as a dashed line.

The equations show a shift in critical temperature and pressure with respect to those of the bulk equation.

III. RESULTS

The vdW equations (9) and (10) give the components of the pressure tensor for a confined fluid in a square section pore of infinite length. At given temperature and density (Fig. 2) we have a homogeneous fluid with different axial and transverse pressures $p_{zz}^* < p_{xx}^*$. On lowering the temperature, maintaining the transverse section constant, a loop appears for the axial component of the pressure (Fig. 3). Here, as in the bulk, phase equilibrium occurs with an xy interface separating a homogeneous gas from a homogeneous liquid (capillary transition). Each region is consistent with the uniformity constraint used to obtain the vdW equations. Then, by applying Maxwell's construction on the isotherm $p_{zz}^* - v^*$, we get for the gas-liquid equilibrium $p_{zzl}^* = p_{zzg}^*$, v_l^* , v_g^* , and $p_{xxl}^* > p_{xxg}^*$. At a lower temperature, the transverse component of the pressure p_{xx}^* also presents a loop (Fig. 4). This loop does not imply a new phase separation, given that in the derivation of the vdW equations the fluid was constrained to be uniform on the scale of the pore transverse

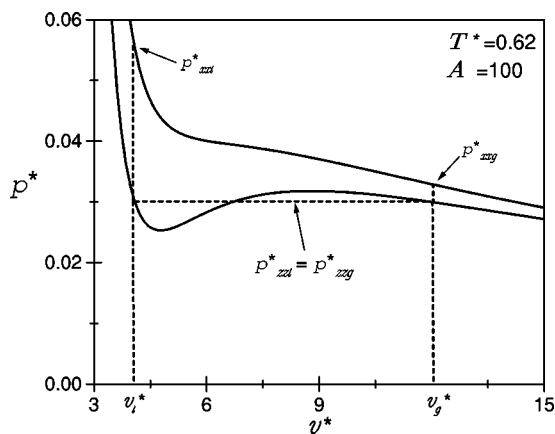


FIG. 3. Capillary condensation for $T^* = 0.62$. The Maxwell construction is used to obtain the gas-liquid coexistence line.

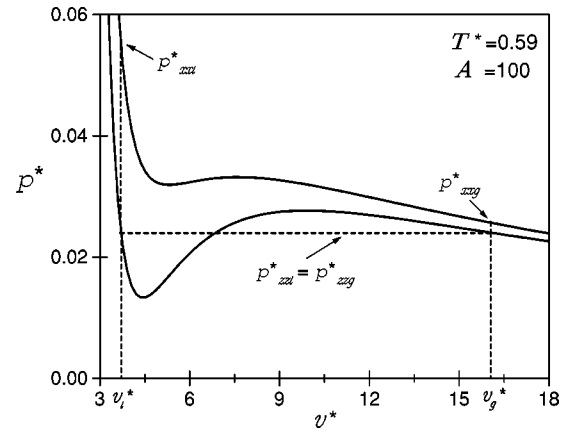


FIG. 4. As Fig. 3, for $T^* = 0.59$.

size; all the states represented by the loop are possible [17]. Thus we still have a phase equilibrium characterized by the axial component of the pressure, as in the case represented in Fig. 3. In Fig. 5 the phase diagrams for two pores of different sizes and for the bulk fluid are shown. Lattice models and numerical simulations [18,14] show a similar behavior, although in these works the wall-fluid interaction was included. For a wall-fluid attractive interaction the critical density is shifted to higher values relative to its bulk value, whereas for repelling walls it is shifted in the opposite direction [18]. In our work the fluid-wall interaction is not taken into account, so the critical density remains the same as in the bulk.

In Table I, we compare the values of the critical temperature with experimental results in a mesoporous siliceous honeycomb-type lattice (MCM-41) [19]. It is worth mentioning that Table I was computed without any adjustment of the parameters a^* , b^* , c_1 , and c_2 , whose values were given above. The results are very good for Ar and N_2 , and acceptable for O_2 , C_2H_4 , and CO_2 .

IV. DISCUSSION

In this paper we have generalized the van der Waals bulk equation for a fluid confined in a nanopore with inert walls.

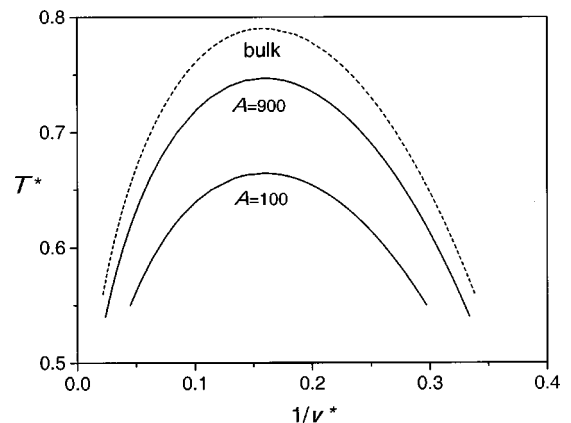


FIG. 5. Phase diagrams for two pore sections (full lines) and for the bulk fluid.

TABLE I. Critical temperature versus the pore radius. The values in parentheses are experimental critical values [19], and each r_{pore} is an average pore radius in a mesoporous MCM-41 molecular sieve. The square section area A in T_c^* was equated to the area corresponding to the experimental cylindrical pore πr_{pore}^2 . The values of T_c were calculated using Eq. (13) with averaged Lennard-Jones parameters [20].

r_{pore} (nm)	T_c (K)				
	Ar	N ₂	O ₂	C ₂ H ₄	CO ₂
1.2	71.7	52.5	64.3 (<71)	109.8 (<142)	111.3 (<161)
1.4	74.8 (74)	55.0 (<61)	67.2 (76)	116.3 (<142)	117.3 (173)
1.8	79.1 (87)	58.5 (68)	71.2 (91)	125.3 (148)	125.7 (195)
2.1	81.3 (>86)	60.3 (76)	73.3 (>92)	129.9 (163)	130.0 (>197)

Confinement of a system of interacting particles makes the components of the force on a given particle different. This idea used in the standard derivation of the van der Waals equation gives the components of the pressure tensor [Eqs. (11) and (12)] for a square section nanopore of infinite length. The equations predict capillary transitions and a shift of the critical parameters with respect to those of the bulk equation. These results are in agreement with the behavior shown by lattice models and numerical simulations. The predicted critical temperatures, displayed in Table I, are in good agreement with experimental data, specially for spherical type particles like Ar. It must be pointed out that the values

were calculated without any adjustment of the equation parameters. The confined van der Waals fluid theory seems to work better than the bulk one. This may be due to the fact that the higher virial contributions not considered in either theory are less important in the confined fluid than in the bulk.

ACKNOWLEDGMENTS

This work was partially supported by CICPBA, Universidad Nacional de La Plata and by the Agencia Nacional de Promoción Científica y Tecnológica (ANPCyT) through Grant No. PICT 03-4517.

-
- [1] R. Evans, *J. Phys.: Condens. Matter* **2**, 8989 (1990).
[2] *Characterization of Porous Solids*, edited by K. K. Unger, J. Rouquerol, K. S. W. Sing, and H. Kral (Elsevier, Amsterdam, 1988).
[3] B. Alberts, D. Bray, J. Lewis, M. Raff, K. Roberts, and J. D. Watson, *Molecular Biology of the Cell* (Garland, New York, 1989).
[4] M. M. Dubinin, in *The Modern Theory of Capillarity*, edited by F. C. Goodrich and A. I. Rusanov (Akademie-Verlag, Berlin, 1981), p. 63.
[5] L. Bonnetain, J. L. Ginoux, and M. Cabedo, in *Characterization of Porous Solids* (Ref. [2]), p. 223.
[6] N. Samid-Merzel, S. G. Lipson, and D. S. Tannhauser, *Phys. Rev. E* **57**, 2906 (1998).
[7] *Fundamentals of Friction: Macroscopic and Microscopic Processes*, edited by I. L. Singer and H. M. Pollock (Kluwer, Dordrecht, 1991).
[8] J. N. Israelachvili, in *Fundamentals of Friction: Macroscopic and Microscopic Processes* (Ref. [7]), p. 351.
[9] P. McGuiggan and J. N. Israelachvili, *J. Mater. Res.* **5**, 2232 (1990).
[10] F. Varnik, J. Baschnagel, and K. Binder, *J. Chem. Phys.* **113**, 4444 (2000).
[11] V. Pot, C. Appert, A. Melayah, D. H. Rothman, and S. Zaleski, *J. Phys. II* **6**, 1517 (1996).
[12] F. Kremer, A. Huwe, M. Arndt, P. Behrens, and W. Schwieger, *J. Phys.: Condens. Matter* **11**, A175 (1999).
[13] M. Thommes and G. H. Findenegg, *Langmuir* **10**, 4270 (1994).
[14] A. Z. Panagiotopoulos, *Mol. Phys.* **62**, 701 (1987).
[15] M. Sliwinska-Bartkowiak, S. L. Sowers, and K. E. Gubbins, *Langmuir* **13**, 1182 (1997).
[16] L. Landau and E. Lifshitz, *Teoría de la Elasticidad* (Reverté, Barcelona, 1969).
[17] J. S. Rowlinson and B. Widom, *Molecular Theory of Capillarity* (Oxford University Press, New York, 1982).
[18] E. V. Votyakov, Yu. K. Tovbin, J. M. D. MacElroy, and A. Roche, *Langmuir* **15**, 5713 (1999).
[19] K. Morishige, H. Fujii, M. Uga, and D. Kinukawa, *Langmuir* **13**, 3494 (1997).
[20] J. O. Hirschfelder, C. F. Curtiss, and R. B. Bird, *Molecular Theory of Gases and Liquids* (Wiley, New York, 1964).